J|A|C|S
ARTICLES
Published on Web 03/20/2002

Computational Studies of Tungsten-Catalyzed *endo*-Selective Cycloisomerization of 4-Pentyn-1-ol

Yinghong Sheng, Djamaladdin G. Musaev,* K. Subba Reddy, Frank E. McDonald, and Keiji Morokuma*

Contribution from the Cherry L. Emerson Center for Scientific Computation and Department of Chemistry, Emory University, Atlanta, Georgia 30322

Received December 3, 2001

Abstract: *Endo*- and *exo*-cycloisomerizations of 4-pentyn-1-ol have been studied computationally with density functional theory, in conjunction with double-ζ and triple-ζ basis sets, both in the absence and in the presence of tungsten carbonyl catalyst. In the absence of the catalyst, both *endo*- and *exo*-cycloisomerizations have been calculated to have a very high activation barrier of ~50−55 kcal/mol and cannot take place. With tungsten pentacarbonyl catalyst, *endo*-cycloisomerization becomes a complex multiple-step reaction and proceeds with a rate-determining barrier of 26 kcal/mol at the $C_\alpha \rightarrow C_\beta$ hydride migration step to form a vinylidene intermediate. The primary role of the tungsten catalyst is to stabilize the vinylidene intermediate, thus lowering the rate-determining barrier. The second important role of the tungsten catalyst in *endo*-cycloisomerization is to assist the OH hydride migration to C_α by making it a multistep process with small activation barriers. The *exo*-cycloisomerization with the catalyst still has a high rate-determining barrier of 47 kcal/mol. These findings clearly explain the experimentally observed *endo*-selectivity in the cycloisomerization of 4-pentyn-1-ol derivatives and support the experimentally proposed mechanism.

1. Introduction

The invention of new chemical transformations is an extraordinarily fertile area of research in synthetic chemistry, and its contributions will facilitate explorations of novel strategies for efficient synthetic access to compounds of commercial and academic importance. The *endo*-selective cycloisomerization of nucleophiles tethered to terminal alkynes is one of those such important reaction types,[1] and the cycloisomerization of alkynyl alcohols has been utilized in efficient syntheses of antiviral nucleosides,[2] polycyclic ethers,[3] and oligosaccharides.[4]

This novel cycloisomerization transformation has been proposed to proceed via a formation of vinylidene intermediate formed by a formal 1,2-shift of the alkyne hydrogen from C_α to C_β.[5] In the metal-free state, the lifetime of vinylidene is extremely short.[6] However, the formation and stabilization of vinylidene intermediate at a transition metal center have been used as a general method for the generation of oxacyclic Fischer carbene products,[7] including five-, six-, and seven-membered products.[8] Chromium, molybdenum, and tungsten pentacarbonyls have been developed as metal catalysts for cycloisomerization of terminal alkynes that are tethered to alcohols, as well as nitrogen, carbon, and sulfur nucleophiles.[9]

Scheme 1

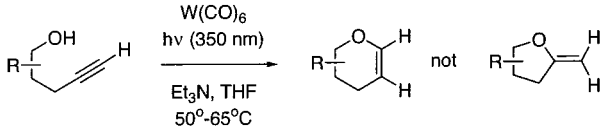

Although molybdenum pentacarbonyl catalyst was initially developed for alkynol cycloisomerization, this catalyst is largely limited to the formation of five-membered ring products.[10] More recently a tungsten pentacarbonyl-catalyzed procedure has been developed for the effective cycloisomerization of alkynyl alcohols to yield six-membered ring products.[11] For instance, *endo*-cycloisomerization of substituted 4-alkyn-1-ol is catalyzed by $W(CO)_6$ when the reactants are photolyzed at 350 nm at or near the reflux point of THF in the presence of triethylamine (Scheme 1). This transformation proceeds with complete

* To whom correspondence should be addressed. E-mail: morokuma@emory.edu.

(1) McDonald, F. E. *Chem.-Eur. J.* **1999**, *5*, 3103.
(2) (a) McDonald, F. E.; Gleason, M. M. *Angew. Chem., Int. Ed. Engl.* **1995**, *34*, 350. (b) McDonald, F. E.; Gleason, M. M. *J. Am. Chem. Soc.* **1996**, *118*, 6648.
(3) Bowman, J. L.; McDonald, F. E. *J. Org. Chem.* **1998**, *63*, 3680.
(4) (a) McDonald, F. E.; Zhu, H. Y. H. *J. Am. Chem. Soc.* **1998**, *120*, 4246. (b) McDonald, F. E.; Reddy, K. S. *Angew. Chem., Int. Ed.* **2001**, *40*, 3653.
(5) Bruce, M. I. *Chem. Rev.* **1998**, *98*, 2797.
(6) Stanton, J. F.; Gauss, J. *J. Chem. Phys.* **1994**, *101*, 3001 and reference therein.
(7) (a) Mills, O. S.; Redhouse, A. D. *Chem. Commun.* **1966**, 444. (b) Mills, O. S.; Redhouse, A. D. *J. Chem. Soc.* **1968**, 1282. (c) Werner, H. *J. Organomet. Chem.* **1994**, *475*, 45. (d) Bruce, M. I. *Chem. Rev.* **1991**, *91*, 197.
(8) (a) Chisholm, M. H.; Clark, H. C. *J. Am. Chem. Soc.* **1972**, *94*, 1532. (b) Bruce, M. I.; Swincer, A. G.; Thomson, B. J.; Wallis, R. C. *Aust. J. Chem.* **1980**, *33*, 2605. (c) Bianchini, C.; Marchi, A.; Mantovani, N.; Marvelli, L.; Masi, D.; Peruzzini, M.; Rossi, P. *Eur. J. Inorg. Chem.* **1998**, 211.
(9) (a) McDonald, F. E.; Chatterjee, A. K. *Tetrahedron Lett.* **1997**, *38*, 7687. (b) McDonald, F. E.; Olson, T. C. *Tetrahedron Lett.* **1997**, *38*, 7691. (c) McDonald, F. E.; Burova, S. A.; Huffman, L. G., Jr. *Synthesis* **2000**, *7*, 970.
(10) (a) McDonald, F. E.; Connolly, C. B.; Gleason, M. M.; Towne, T. B.; Treiber, K. D. *J. Org. Chem.* **1993**, *58*, 6952. (b) McDonald, F. E.; Zhu, H. Y. H. *Tetrahedron* **1997**, *53*, 11061.
(11) (a) McDonald, F. E.; Reddy, K. S.; Díaz, Y. *J. Am. Chem. Soc.* **2000**, *122*, 4304. (b) McDonald, F. E.; Reddy, K. S. *J. Organomet. Chem.* **2001**, *617*, 446.

Scheme 2. Mechanism of the Catalytic, *endo*-Selective Alkynol Cycloisomerization Reaction, Proposed in Ref 11 and Modified in This Paper

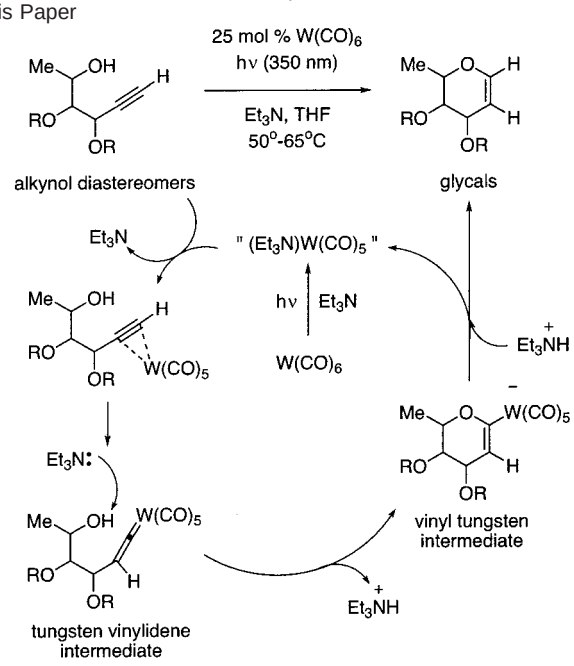

endo-regioselectivity provided that the reaction is conducted under strictly anaerobic (oxygen-free) conditions.

The previously hypothesized mechanism of cycloisomerization of terminal alkynyl alcohols involves an initial rearrangement of an η^2 metal-alkyne complex to a vinylidene complex.[11] Base-induced cyclization of the alcohol nucleophile might afford the cyclic anionic vinyl tungsten intermediate, and its protonation leads to the endocyclic enol ether product (Scheme 2). In the present paper, we present the results of computational studies on the cycloisomerization of 4-pentyn-1-ol. The purposes of our study are as follows: (1) to investigate the mechanisms of cycloisomerization in the absence and presence of tungsten catalyst; (2) to investigate the geometrical features of the transition structure, intermediates, and products of cycloisomerization; (3) to analyze the role of the tungsten catalyst in enhancing the reactivity of cycloisomerization; and (4) to investigate the factors responsible for the regioselectivity of *endo*- versus *exo*-cycloisomerization.

2. Methods of Calculation

We used the parent 4-pentyn-1-ol as the substrate, initially studying its cycloisomerization reaction without tungsten carbonyl catalyst. Two different unimolecular cycloisomerization reactions of 4-pentyn-1-ol were investigated (Scheme 3); pathway A is *endo*-cycloisomerization which leads to a six-membered ring product, and pathway B leads to a five-membered ring product via *exo*-cycloisomerization. We subsequently studied the mechanism of cycloisomerization of 4-pentyn-1-ol in the presence of tungsten catalyst.

All calculations were performed using the hybrid B3LYP density functional method, which uses Becke's 3-parameter nonlocal exchange functional[12] mixed with the exact (Hartree−Fock) exchange functional and Lee−Yang−Parr's nonlocal correlation functional.[13] Geometries of all the reactants, intermediate, and transition states were optimized without any constraint with the analytical gradient using the Lanl2dz basis set,[14] which combines the Hay−Wadt relativistic effective core

Scheme 3

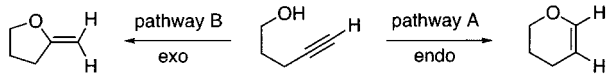

potential for W with a valence double-ζ basis set. Harmonic vibration frequencies were calculated analytically for each optimized transition state (TS) structure to confirm that this is a true TS (the number of imaginary frequency Nimag = 1). Intrinsic reaction coordinate (IRC) or pseudo-IRC (optimization after a step on IRC) calculations were performed for some of the TSs to confirm the reactants and the products these TSs connect to. The improved were recalculated energies for all the B3LYP/lanl2dz optimized geometries with the Stuttgart/Dresden ECP + SDD basis set for W and the 6-31G** basis set for the other atoms. Previously,[15] it was demonstrated that the B3LYP method with double-ζ quality basis sets, such as lanl2dz, for geometry optimization, and triple-ζ quality basis sets, such as SDD, for relative energy calculations, provide reasonable agreement with available experimental data and high level methods, while this tends to underestimate the calculated barriers by a few kcal/mol.[16] In this paper we mostly discuss the obtained chemical trends and relative energies, thus we believe that the underestimation of the calculated barriers by 3−5 kcal/mol at the B3LYP/SDD level will not affect our conclusions.

All calculations were carried out with the Gaussian 98 program.[17]

3. Results and Discussion

A. Metal-Free Cycloisomerizations. *endo*-Cycloisomerization of 4-Pentyn-1-ol. The optimized structures and energies of the reactants, intermediates, TSs, and products of *endo*-cycloisomerization of 4-pentyn-1-ol **1** are shown in Figure 1. We find that the key intermediate for this reaction is a cyclic vinylidene intermediate **N4**, where the O−C_α distance formed by interaction of alkoxyl O with the vinylidene terminal carbon C_α is 1.88 Å, indicating that the O−C_α bond formation is not yet complete. This key intermediate **N4** can be reached from the reactant **1** via two different pathways. In the first pathway, the hydride migration from the terminal carbon C_α to C_β of alkyne and the O−C_α ring closure take place concertedly, in a

(12) Becke, A. D. *J. Chem. Phys.* **1993**, *98*, 5648.
(13) Lee, C.; Yang, W.; Parr, R. G. *Phys. Rev. B* **1988**, *37*, 785.
(14) (a) Dunning, T. H., Jr.; Hay, P. J. In *Modern Theoretical Chemistry*; Schaefer, H. F., III, Ed.; Plenum: New York, 1976; pp 1−28. (b) Hay, P. J.; Wadt, W. R. *J. Chem. Phys.* **1985**, *82*, 270. (c) Wadt, W. R.; Hay, P. J. *J. Chem. Phys.* **1985**, *82*, 284. (d) Hay, P. J.; Wadt, W. R. *J. Chem. Phys.* **1985**, *82*, 299.
(15) (a) Cui, Q.; Musaev, D. G.; Svensson, M.; Sieber, S.; Morokuma, K. *J. Am. Chem. Soc.* **1995**, *117*, 12366. (b) Musaev, D. G.; Morokuma, K. *J. Phys. Chem.* **1996**, *100*, 6509. (c) Erikson, L. A.; Pettersson, L. G. M.; Siegbahn, P. E. M.; Wahlgren, U. *J. Chem. Phys.* **1995**, *102*, 872. (d) Ricca, A.; Bauschlicher, C. W., Jr. *J. Phys. Chem.* **1994**, *98*, 12899. (e) Heinemann, C.; Hertwig, R. H.; Wesendrup, R.; Koch, W.; Schwarz, H. *J. Am. Chem. Soc.* **1995**, *117*, 495. (f) Hertwig, R. H.; Hrusak, J.; Schroder, D.; Koch, W.; Schwarz, H. *Chem. Phys. Lett.* **1995**, *236*, 194. (g) Schroder, D.; Hrusak, J.; Hertwig, R. H.; Koch, W.; Schwerdtfeger, P.; Schwarz, H. *Organometallics* **1995**, *14*, 312. (h) Fiedler, A.; Schroder, D.; Shaik, S.; Schwarz, H. *J. Am. Chem. Soc.* **1994**, *116*, 10734. (i) Fan, L.; Ziegler, T. *J. Chem. Phys.* **1991**, *95*, 7401. (j) Berces, A.; Ziegler, T.; Fan, L. *J. Phys. Chem.* **1994**, *98*, 1584. (k) Lyne, P. D.; Mingos, D. M. P.; Ziegler, T.; Downs, A. J. *Inorg. Chem.* **1993**, *32*, 4785. (l) Li, J.; Schreckenbach, G.; Ziegler, T. *J. Am. Chem. Soc.* **1995**, *117*, 486.
(16) (a) Lynch, B. J.; Fast, P. L.; Harris, M.; Truhlar, D. G. *J. Phys. Chem. A* **2000**, *104*, 4811. (b) Bach, R. D.; Glukhovtsev, M. N.; Canepa, C. *J. Am. Chem. Soc.* **1998**, *120*, 775.
(17) Frisch, M. J.; Trucks, G. W.; Schlegel, H. B.; Scuseria, G. E.; Robb, M. A.; Cheeseman, J. R.; Zakrzewski, V. G.; Montgomery, J. A., Jr.; Stratmann, R. E.; Burant, J. C.; Dapprich, S.; Millam, J. M.; Daniels, A. D.; Kudin, K. N.; Strain, M. C.; Farkas, O.; Tomasi, J.; Barone, V.; Cossi, M.; Cammi, R.; Mennucci, B.; Pomelli, C.; Adamo, C.; Clifford, S.; Ochterski, J.; Petersson, G. A.; Ayala, P. Y.; Cui, Q.; Morokuma, K.; Malick, D. K.; Rabuck, A. D.; Raghavachari, K.; Foresman, J. B.; Cioslowski, J.; Ortiz, J. V.; Stefanov, B. B.; Liu, G.; Liashenko, A.; Piskorz, P.; Komaromi, I.; Gomperts, R.; Martin, R. L.; Fox, D. J.; Keith, T.; Al-Laham, M. A.; Peng, C. Y.; Nanayakkara, A.; Gonzalez, C.; Challacombe, M.; Gill, P. M. W.; Johnson, B. G.; Chen, W.; Wong, M. W.; Andres, J. L.; Head-Gordon, M.; Replogle, E. S.; Pople, J. A. *Gaussian 98*, revision A.7; Gaussian, Inc.: Pittsburgh, PA, 1998.

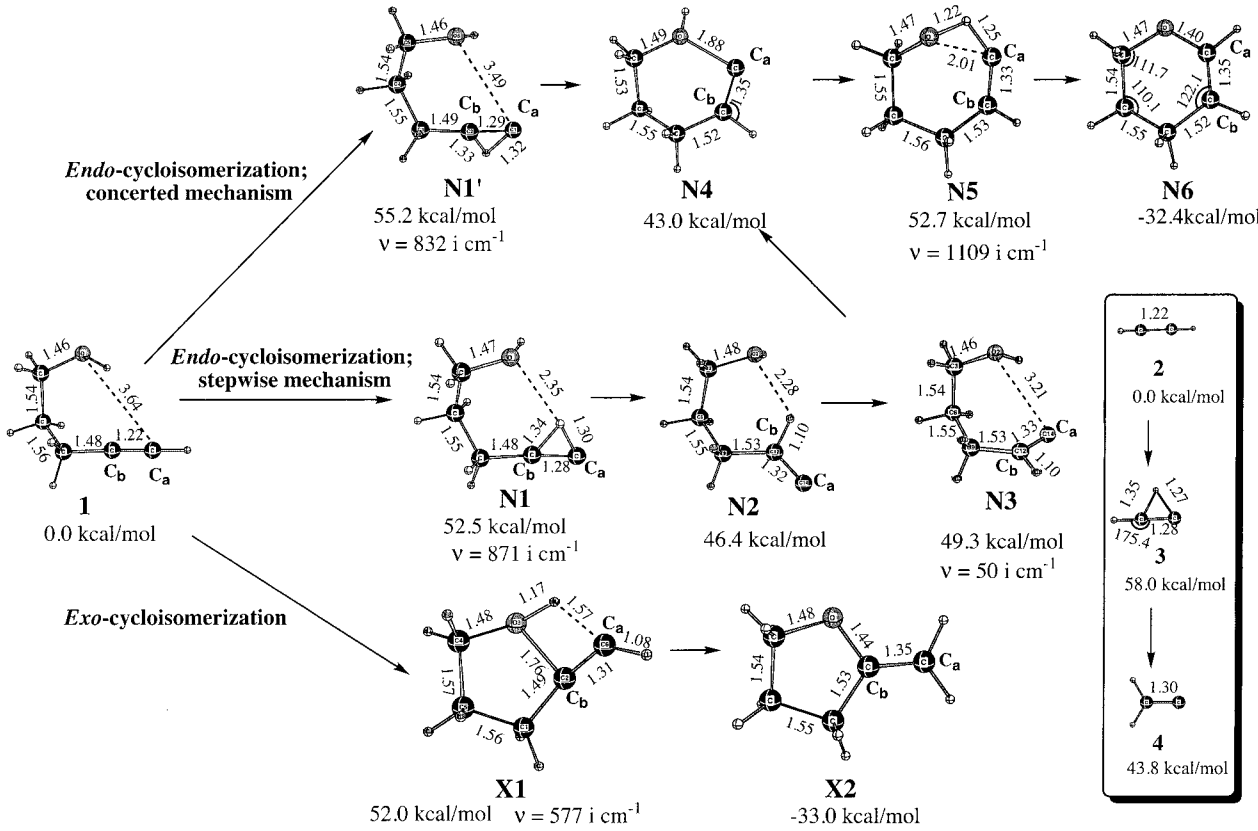

Figure 1. The optimized stationary state structures (in Å and deg) and relative energies (relative to **1**) of metal-free *endo*- and *exo*-cycloisomerization pathways of 4-pentyn-1-ols. For comparison, the hydride migration in acetylene is also illustrated.

single step, via the transition state (TS) **N1′**. The activation barrier corresponding to this process is found to be 55.2 kcal/mol. It is important to note that in this path the hydride moves from C_α to C_β on the side opposite to the alkoxyl group. The second, stepwise pathway starts with the hydride migration from C_α to C_β; this time the hydride ligand moves on the same side with the alkoxyl group. The TS, **N1**, corresponding to this process has a short O···HC$_\alpha$ distance (2.35 Å), indicating weak hydrogen bonding with the alkoxyl group. The frequency calculation confirms the nature of this transition state; we found one imaginary frequency of 871*i* cm^{-1} corresponding to the hydride migration. In addition, an IRC calculation shows that **N1** connects the reactant **1** with the open vinylidene intermediate **N2**. In **N2**, the weak O···HC hydrogen bond is retained with the O···H distance of 2.28 Å. The energetic barrier associated with TS **N1** is 52.5 kcal/mol. The process **1** → **N1** → **N2** is found to be endothermic by 46.4 kcal/mol.

The next step of the reaction is the ring closure (O···C$_\alpha$ bond formation), which occurs simultaneously with the rotation of the C$_\beta$(H)C$_\alpha$ group around the C$_\gamma$−C$_\beta$ bond. In the TS **N3** for this process, the O and C$_\alpha$ atoms start to interact to close the ring with the O···C$_\alpha$ distance of 3.21 Å. The normal coordinate analysis confirms that **N3** is a real TS with one imaginary frequency of 50*i* cm^{-1}. IRC calculations indicate that TS **N3** connects intermediate **N2** with the key intermediate **N4**, which was discussed above. The barrier at TS **N3** is only 2.9 kcal/mol relative to **N2**. The process **N2** → **N3** → **N4** is exothermic by 3.4 kcal/mol. Overall, the rate-determining barrier of the stepwise pathway at TS **N1** is found to be slightly (2.7 kcal/mol) lower than that for the concerted pathway at TS **N1′**.

A comparison of the calculated energetics for the hydride migration process in 4-pentyn-1-ol, **1**, and the acetylene[18] molecule, **2** (see Figure 1), shows that the rate-determining barrier for hydride migration for **1** is lower by 5.5 kcal/mol than that for acetylene **2** → **3**, 58.0 kcal/mol. This result could be rationalized in terms of the hydrogen-bonding interaction with the hydroxyl group in 4-pentyn-1-ol.

From the cyclic vinylidene intermediate **N4**, the *endo*-cycloisomerization of 4-pentyn-1-ol proceeds with the hydride migration from the hydroxyl to the terminal vinylidene carbon accompanied with the completion of ring closure or C−O bond formation. This process occurs through the TS **N5** and leads to the six-membered *endo* product **N6**. At TS **N5**, the hydride ligand is located nearly at the equal distance from C$_\alpha$ and O, the two atoms between which migration is taking place, and the O···C$_\alpha$ distance is stretched from 1.88 Å in **N4** to 2.01 Å in **N5**. The activation barrier for this process is calculated to be 9.7 kcal/mol. The normal coordinate analysis shows that **N5** is a real TS with one imaginary frequency, 1109*i* cm^{-1}, corresponding to hydride migration and C$_\alpha$−O bond formation. IRC calculation confirmed that TS **N5** connects **N4** with **N6**. The product **N6**, where C−O bond formation and hydride migration from O to C is completed, is much lower in energy (75.4 kcal/mol) than reactant **N4**. The entire reaction of the *endo*-cycloisomerization of 4-pentyn-1-ol, proceeding from **1** to **N6**, is found to be exothermic by 32.4 kcal/mol.

***exo*-Cycloisomerization of 4-Pentyn-1-ol.** Now, let us discuss the *exo*-cycloisomerization of 4-pentyn-1-ol leading to the five-membered ring molecule **X2**. This process is found to

(18) Jursic, B. S. *J. Mol. Struct.* **1999**, *488*, 87.

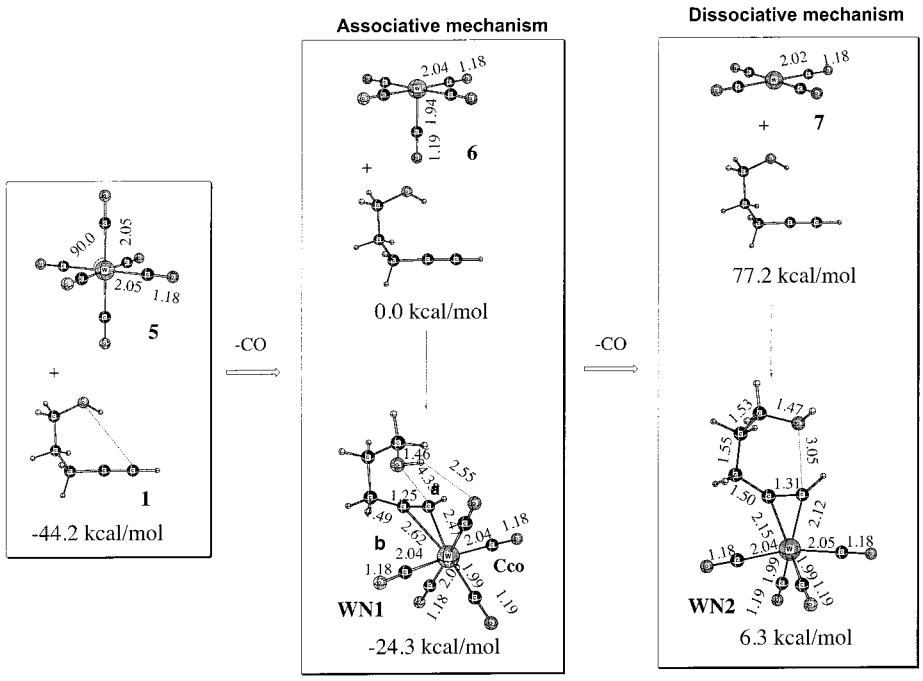

Figure 2. The optimized stationary state structures (in Å and deg) and relative energies of $W(CO)_6$ (**5**), $W(CO)_5$ (**6**), and $W(CO)_4$ (**7**), and their adduct complexes with 4-pentyn-1-ol.

be a single-step reaction proceeding via a concerted TS **X1**, as seen in Figure 1. In **X1**, the hydride ligand that should migrate from the hydroxyl to the terminal carbon is still closer to the hydroxyl O; the O−H and C_α−H distances are 1.17 and 1.57 Å, respectively. Meanwhile, the terminal C−C bond is stretched from 1.22 Å in the reactant **1** to 1.31 Å in **X1**. The hydroxyl oxygen and C_β atoms approach each other with an O−C_β distance of 1.76 Å. Note that the change of the angle H−C_α−C_β from 180° in **1** to 131.4° in **X1** indicates a significant change in hybridization of the C_α atom, from sp to sp^2, similar to that in the *exo* product **X2**, and suggests a rather asynchronous character of this concerted TS. The normal coordinate analysis shows that **X1** is a real TS with only one imaginary frequency of 577*i* cm^{-1}, with the reaction coordinate consisting of several geometrical parameters corresponding to hydride migration from O to C_α and O−C_β bond formation. IRC calculations confirm that this TS connects **1** with **X2**. The activation barrier at **X1** is calculated to be 52.0 kcal/mol, very much comparable to that for the *endo*-cycloisomerization process discussed above. The entire process of *exo*-cycloisomerization of 4-pentyn-1-ol, **1** → **X1** → **X2**, is calculated to be 33.0 kcal/mol exothermic. The stability of the *exo*-cycloisomerization product **X2** is very similar to that of the *endo*-cycloisomerization product **N6**.

Thus, in the absence of catalyst, the activation barriers for both *endo*- and *exo*-cycloisomerization of 4-pentyn-1-ol are very large, greater than 50 kcal/mol. Therefore, one may conclude that neither *endo*- nor *exo*-cycloisomerization reactions of 4-pentyn-1-ol can take place under mild conditions in the absence of catalyst.

B. Metal-Catalyzed Cycloisomerizations. In the preceding subsection we have demonstrated that neither *endo*- nor *exo*-cycloisomerization reaction of 4-pentyn-1-ol can occur without catalyst. However, various transition metal complexes can effectively catalyze the cycloisomerization of alkynyl alcohol substrates.[2,4,10,11] The detailed mechanism of these catalytic processes, as well as the factors affecting the mechanism of these reactions, still remains unclear. Herein we elucidate the mechanism of cycloisomerization reaction of 4-pentyn-1-ol catalyzed by tungsten carbonyl.[11] In our studies, we will explore the mechanism proposed by McDonald and co-workers.[11] According to this mechanism, the initial step of the reaction is dissociation of a CO-ligand from the tungsten hexacarbonyl to produce catalytically active tungsten pentacarbonyl. In the following steps, the alkyne coordinates to the W center, and the hydride migration gives a tungsten-vinylidene intermediate, which undergoes regioselective nucleophilic addition to the terminal carbon, and produces a vinyl tungsten intermediate (Scheme 2). We begin our discussions from the initial steps of the reaction: CO dissociation from $W(CO)_6$ and alkyne coordination to the coordinatively unsaturated tungsten complex.

Generation of Active Catalyst by CO Elimination. The structures associated with the initial steps of the proposed[11] mechanism of the $W(CO)_6$ (**5**)-catalyzed 4-pentyn-1-ol cycloisomerization reaction are shown in Figure 2. As was mentioned in the Introduction, the *endo*-cycloisomerization of substituted 4-pentyn-1-ol was initiated experimentally by photolysis of the reactants at 350 nm. We believe that when the stable $W(CO)_6$ **5** is photolyzed, the catalytically active complex $W(CO)_5$ **6** is formed. Our calculations show that the dissociation of one carbonyl ligand from $W(CO)_6$ is endothermic by 44.2 kcal/mol. Further photolytic (or thermal) elimination of CO from $W(CO)_5$ would give $W(CO)_4$, which can also be an active catalyst that will initiate what could be called a dissociative mechanism. However, our calculations in Figure 2 show that the dissociation of the second CO is highly endothermic (77.2 kcal/mol), and the resultant coordinatively highly unsaturated $W(CO)_4$ **7** is unlikely to be stable under the experimental conditions.[11] In a solvent such as THF, this species will surely be solvated and stabilized with THF in the first coordination sphere. Considering a substantially higher second CO dissociation energy, and a higher relative energy of the alkyne adduct **WN2** as compared to the adduct **WN1**, formed upon alkyne coordination to

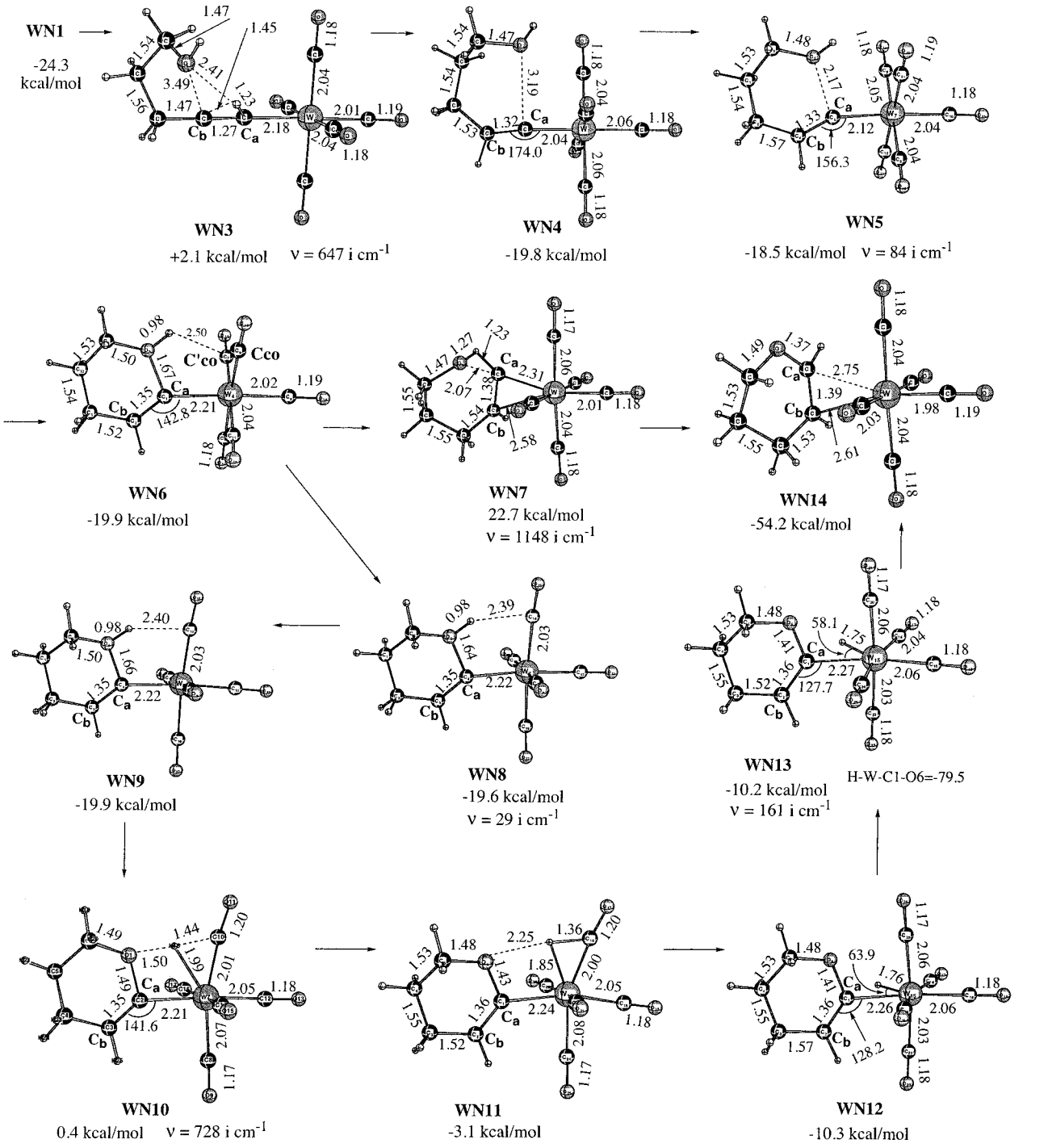

Figure 3. The optimized stationary point structures (in Å and deg) and relative energies (relative to $W(CO)_5$ + **1**) on the reaction pathways of *endo*-cycloisomerization of 4-pentyn-1-ol in the presence of the $W(CO)_5$ catalyst.

$W(CO)_4$ and $W(CO)_5$, respectively, one may safely conclude that the dissociative mechanism is not likely to contribute to the overall rate. Therefore, only the associative mechanism initiated by $W(CO)_5$ will be discussed.

***endo*-Cycloisomerization of 4-Pentyn-1-ol Catalyzed by $W(CO)_5$ Complex.** Thus, the catalytic reaction is initiated by pentacarbonyl tungsten **6**. The optimized structures for the reactants, intermediates, transition states, and products of *endo*-cycloisomerization of 4-pentyn-1-ol in the presence of tungsten pentacarbonyl catalyst are shown in Figure 3. The coordination of 4-pentyn-1-ol substrate **1** to pentacarbonyl tungsten **6** initially results in formation of π-alkyne-$W(CO)_5$ adduct **WN1**, as discussed above and shown in Figure 2. In **WN1**, the hydroxyl group of the 4-pentyn-1-ol ligand forms a weak hydrogen bond with one of the carbonyl oxygen atom with OH···OC = 2.55 Å. The adduct formation process **1** + **6** → **WN1** is calculated to be 24.3 kcal/mol exothermic.

For comparison, we also have studied the adduct formation between acetylene and $W(CO)_5$ (calculated structures are shown in Figure S1 of the Supporting Information). Comparison of the acetylene-$W(CO)_5$ complex **8** and **WN1** shows that in **8** the C≡C triple bond is symmetrically coordinated to the W

center with the two equal W−C distances of 2.43 Å, while in **WN1** the two W−C (C≡C) distances are different, 2.47 and 2.62 Å. Also, the $C_\alpha-C_\beta-W-C_{CO}$ dihedral angle in **WN1** is 13.7°, which is zero in **8**. These geometrical differences are results of the electronic and steric effects from the substituents, $(CH_2)_3OH$ in 4-pentyn-1-ol versus H in acetylene.

From the 4-pentyn-1-ol $W(CO)_5$ π-complex **WN1**, the calculation shows that the reaction proceeds via hydride migration from C_α to C_β, leading to the tungsten alkylidene complex **WN4**. The TS **WN3** for this process, given in Figure 3, has one imaginary frequency ($647i$ cm^{-1}) corresponding to the motion of H from C_α to C_β. In addition, the pseudo IRC calculation indicates that **WN3** connects the π-complex **WN1** with the alkylidene complex **WN4**. As seen in Figure 3, upon going from **WN1** to TS **WN3**, migration of H from C_α to C_β is in progress, while the $W-C_\beta$ bond is broken, and the $W-C_\alpha$ bond becomes stronger. The $W-C_\alpha$ bond distance is calculated to be 2.47 and 2.18 Å in **WN1** and **WN3**, respectively. The geometrical parameters of the 4-pentyn-1-ol fragment in TS **WN3** are similar to those in TS **N1** for the isomerization of 4-pentyn-1-ol without catalyst (see Figure 1), except for the $C_\alpha-H$ and $C_\beta-H$ bond distances; the $C_\alpha-H$ bond distance is 1.23 Å in **WN3**, which is 0.07 Å shorter than 1.30 Å in **N1**, while the $C_\beta-H$ bond distance of 1.45 Å in **WN3** is longer than 1.34 Å in **N1**. These geometrical differences indicate that the hydride migration of TS **WN3** in the presence of catalyst is earlier than that of **N1** without catalyst.

The early nature of the TS **WN3** as compared with **N1** is in part dictated by the energetics of the reactions: **WN1** → **WN3** → **WN4** and **N1** → **N3** → **N4**. The reaction with catalyst is calculated to be only slightly (4.4 kcal/mol) endothermic, while it was highly (46.4 kcal/mol) endothermic in the absence of catalyst. This is rationalized by formation of the tungsten-vinylidene complex during the reaction in the presence of catalyst. As seen in Figure 3, the $W-C_\alpha$ bond length in the vinylidene complex **WN4** is 2.04 Å, which lies in the range of a typical metal−carbon double bond distance.[19] The $C_\alpha-C_\beta$ distance changes from 1.25 Å in **WN1** to 1.32 Å in **WN4**, indicating the cleavage of one π-bond of a C≡C triple bond of **WN1** and formation of a C═C double bond in the **WN4**. In other words, **WN4** is a tungsten-vinylidene complex. The $\angle W-C_\alpha-C_\beta$ bond angle is calculated to be 174.0° in **WN4**, while it was found to be linear in its acetylene analogue **10** (Figure S1, Supporting Information). The 6° reduction of $\angle W-C_\alpha-C_\beta$ upon going from **10** to **WN4** is believed to be a result of weak interaction between C_α and O.

The activation barrier for hydride migration in 4-pentyn-1-ol in the presence of tungsten catalyst is found to be 26.4 kcal/mol, which is about 25 kcal/mol lower than without catalyst. Thus, the tungsten catalyst reduces the rate-determining hydride migration barrier by a large amount, making this reaction feasible under mild conditions. This reduction of the barrier is rationalized by the reduced endothermicity of the hydride migration reaction, which is the result of stabilization of the vinylidene intermediate by tungsten−carbon double bond formation.

For comparison, the same barrier in the presence of catalyst for HC≡CH (**8** to **9** in Figure S1) is calculated to be 31.0 kcal/mol, 4.6 kcal/mol higher than that for 4-pentyn-1-ol. As was the case for the reaction without catalyst, this difference in the hydride migration barriers between acetylene and 4-pentyn-1-ol could be explained by the existence of a weak hydrogen bond (2.41 Å) between the $C^\alpha-H$ and the hydroxyl oxygen in **WN3**.

Overall, one may conclude that in the existence of the $W(CO)_5$ catalyst the hydride migration barrier in 4-pentyn-1-ol is dramatically reduced, and the reaction becomes significantly less endothermic, mostly because of formation of a tungsten-vinylidene (W═C bond) complex. This theoretical finding agrees with the previous hypothesis that cycloisomerization proceeds via formation of a tungsten-vinylidene intermediate.[11]

The next step of reaction from the tungsten-vinylidene intermediate **WN4** is expected to be the formation of $C_\alpha-O$ bond, that is, the ring closure. The calculation shows that this process proceeds over the TS **WN5** and leads to the six-membered ring intermediate **WN6**. The calculated geometry of TS **WN5** is similar to that of the reactant intermediate **WN4**. The major difference is reduction of the $O-C_\alpha$ distance from 3.19 Å in **WN4** to 2.17 Å in **WN5**, which is accompanied by elongation of the $W-C_\alpha$ bond distance from 2.04 to 2.12 Å and an increase in the $\angle W-C_\alpha-C_\beta$ angle from 174.0° to 156.3°. The normal coordinate analysis and IRC calculation show that TS **WN5** has only one imaginary frequency ($84i$ cm^{-1}), consisting of the $C_\alpha-O$ bond formation motion, and connects **WN4** with **WN6**. At the product of this step, **WN6**, the $O-C_\alpha$ distance is as short as 1.67 Å; the $O-C_\alpha$ bond formation is nearly completed. The energetic barrier at this TS **WN5**, relative to **WN4**, is small, 1.3 kcal/mol. The ring-closure process, **WN4** → **WN5** → **WN6**, is found to be nearly thermoneutral.

Comparison of the catalyst-free and tungsten-catalyzed ring-closure processes, **N2** → **N3** → **N4** and **WN4** → **WN5** → **WN6**, shows that the latter is slightly more favorable than the former; tungsten catalyst slightly reduces the barrier (from 2.9 to 1.3 kcal/mol) and stabilizes (by 3.5 kcal/mol) the product. However, catalyst-free and tungsten-catalyzed processes have a significant intrinsic difference. The catalyst-free ring-closure process involves the formation of the $C_\alpha-O$ bond using the vacant carbon π-orbital of the C_α center and the p-lone pair of the O center. However, the tungsten-catalyzed ring-closure process involves the π^*-component of the $W=C_\alpha$ double bond of **WN4** and the p-lone pair of the O center to form the $C_\alpha-O$. In other words, during the tungsten-catalyzed ring-closure process the π-component of the $W=C_\alpha$ double bond should be broken to form the $C_\alpha-O$ bond. This could be seen in the calculated $W-C_\alpha$ bond distances; upon going from **WN4** to **WN5** and **WN6** the $W-C_\alpha$ bond distance elongates from 2.04 to 2.12 and 2.21 Å, respectively.

The next step of reaction from the ring-closure product **WN6** is migration of the hydride from the O center to C_α to form the final product **WN14**. We have found that this process may proceed via two different pathways: concerted and stepwise.

The concerted process, **WN6** → **WN7** → **WN14**, proceeds via the TS **WN7**, where simultaneously with the hydride transfer from O to C_α, the η^1-η^2 rearrangement of the $C_\alpha=C_\beta H$ fragment takes place from being bonded to the W center with C_α (η^1) in **WN6** to its coordination to the W center by C_α and C_β (η^2) in **WN14**. The normal-mode analysis shows that **WN7** is a real TS with one imaginary frequency of $1148i$ cm^{-1}, and IRC calculation confirmed that **WN7** connects **WN6** with **WN14**. As seen in Figures 1 and 3, the geometry of the 4-pentyn-1-ol

(19) Frenking, G.; Fröhlich, N. *Chem. Rev.* **2000**, *100*, 717.

fragment in TS **WN7** resembles that in its catalyzed-free analogue **N5**. The 0.02−0.05 Å differences in the O−H, C_α−H, and C_α−C_β bond distances could be rationalized by the involvement of the C_α═C_β fragment to the π-bonding with the W center in **WN7**. This could also be the reason for a high activation barrier, 42.6 kcal/mol, for the tungsten-catalyzed process; for the catalyst-free process this barrier was only 9.7 kcal/mol.

However, the second stepwise pathway from the same **WN6** proceeds almost without activation barrier and leads to another six-membered ring intermediate **WN9**. A barrier of only 0.3 kcal/mol exists at TS **WN8**, separating **WN6** and **WN9**. Comparison of **WN6** and **WN9** shows that they are rotational isomers. In **WN6** the six-membered ring is staggered with the CO ligands; the dihedral angles ∠HO−C_α−W−C_{CO} and ∠HO−C_α−W−C'_{CO} are 41.0° and −50.6°, respectively. However, in **WN9** the six-membered ring is eclipsed with the CO ligands with these dihedral angles of −8.5° and −97.3°, respectively. Therefore, TS **WN8**, connecting these two isomers, is expected to be a TS for rotational isomerization around the W−C_α bond. The normal coordinate analysis and IRC calculation confirmed that TS **WN8** is a TS with a small imaginary frequency (29*i* cm^{-1}), corresponding to the rotation of the six-membered ring around the W−C_α bond, and connects **WN6** and **WN9**. This rotation facilitates the interaction of the hydroxyl hydrogen atom with the carbonyl ligand (the OH···CO distance is found to be 2.40 Å in **WN9**, while it was 2.50 Å in **WN6**), which moves the hydride closer to the tungsten center; the W−H and H−C_{CO} distances are 2.97 and 2.51 Å in **WN6**, and 2.95 and 2.40 Å in **WN9**, respectively.

In the next step from **WN9**, a surprising hydride migration from the O center to the W center (and carbonyl ligand) takes place via the TS **WN10** and leads to the formation of a W-formyl complex, **WN11**. This TS is confirmed to have one imaginary frequency (728*i* cm^{-1}) and connects **WN9** with a product **WN11**. The closer inspection of the geometrical parameters of **WN10** indicates that it is a tungsten-mediated hydride migration TS from the O center to carbonyl ligand. In **WN10** the O−H bond is very much stretched (1.50 Å) as compared to 0.98 Å in **WN9**. Meanwhile, the H−C(carbonyl) and the W−H bond have started to form at 1.44 and 1.99 Å, respectively. As expected, this hydrogen migration strengthens the O−C_α bond; the O−C_α distance is reduced from 1.66 Å in **WN9** to 1.49 Å in TS **WN10**. Other geometrical parameters do not change significantly. These trends in the change of geometrical parameters, O−H, H−C(carbonyl), W−H, and O−C_α bond distances, continue upon going to the product **WN11**, where the O−H bond is completely broken, the H−C(carbonyl) and the W−H bond are already formed at 1.36 and 1.85 Å, respectively, and the O−C_α bond distance is further reduced to 1.43 Å. The activation barrier at **WN10** is calculated 20.3 kcal/mol relative to **WN9**. This is the second highest barrier in the entire mechanism of the *endo*-cycloisomerization reaction. Overall the process **WN9** → **WN11** is found to be endothermic by 16.5 kcal/mol.

The intermediate **WN11** is relatively unstable and easily rearranges to the tungsten-hydride complex **WN12**. Our attempts to locate the TS connecting **WN11** and **WN12** failed and led to either **WN11** or **WN12**. Therefore, we conclude that **WN11** rearranges to **WN12** with a very small activation barrier. Closer comparison of the geometries of **WN11** and **WN12** could explain the reason the barrier between them should be small. Both **WN11** and **WN12** are pentagonal bipyramidal complexes. In both **WN11** and **WN12**, two carbonyl ligands occupy the axial positions, while the hydride, the six-membered ring, and three carbonyl ligands occupy the five equatorial positions, with the bond angles of ∠H−W−C_α = 75.0°, ∠H−W−C_{CO} = 41.0°, ∠C_{CO}−W−C_{CO} = 80.1° and 80.4°, and C_{CO}−W−C_α = 84.9° in **WN11**, and 63.9°, 60.9°, 82.8° and 82.7°, and 69.8° in **WN12**. **WN11** and **WN12** differ from each other mainly in the rotation of six-membered ring. In **WN11**, the O−C_α−W−H dihedral angle is close to zero, while in **WN12**, it is almost 90°. In other words, the rotation of the six-membered ring facilitates the cleavage of the H−C(carbonyl) bond, and gives the W−H bond in **WN12**. **WN12** is more stable by 7.2 kcal/mol than **WN11**. In the **WN6** → **WN9** rearrangement, we have shown above that the rotation around the W−C_α σ-bond takes place with a 0.3 kcal/mol barrier. Therefore, it is not surprising that we could not locate a similar rotational TS separating **WN11** and **WN12**.

The next step of the reaction is formation of the final product complex **WN14**. This could be achieved from **WN12** by migration of the hydride ligand from W to the C_α center. The activation barrier for this step is extremely low, 0.1 kcal/mol, at the TS **WN13** (see Figure 3). The geometry of this TS is very similar to that of **WN12**; the major change occurs in the ∠H−W−C_α angle, which is reduced from 63.9° in **WN12** to 58.1° in **WN13**. This is a very early TS. The normal-mode analysis and IRC calculation confirmed one imaginary frequency (161*i* cm^{-1}) that connects **WN12** and **WN14**. The process **WN12** → **WN13** → **WN14** is found to be highly exothermic (44.0 kcal/mol), which also is consistent with the early character of TS **WN13**. **WN14** is the π-complex of the *endo*-cycloisomerization product with $W(CO)_5$, where the C_α═C_β double bond is coordinated to the W center asymmetrically; W−C_α and W−C_β bond distances are 2.75 and 2.61 Å, respectively. This could be explained with an asymmetric nature of the ligand environment for C_α and C_β. The dissociation of the *endo*-cycloisomerized product from **WN14** regenerates the active catalyst $W(CO)_5$. The calculated dissociation energy of the product from **WN14** is calculated to be 21.8 kcal/mol without including entropy and solvent effects; the entropy effect is expected to reduce this by ca. 10 kcal/mol.

***exo*-Cycloisomerization of 4-Pentyn-1-ol Catalyzed by $W(CO)_5$ Complex.** The mechanism of the *exo*-cycloisomerization of 4-pentyn-1-ol catalyzed by $W(CO)_5$ complex is found to be simple, a single-step reaction. The calculated geometries and energetics of the intermediates and transition states of this process were given in Figure 4.

As in the *endo*-cycloisomerization, the *exo*-cycloisomerization starts with the π-complex **WN1**, proceeds via the concerted TS **WX1**, and leads to the product complex **WX2**. We could not find such a multistep mechanism as was found for *endo*-cycloisomerization. In **WX1**, the hydride migration from the hydroxyl to the terminal carbon C_α, the formation of the O−C_β bond, and the cleavage of the C_α−C_β π-bond all occur simultaneously. As see in Figure 4, in TS **WX1**, the hydride ligand, which should migrate, is still closer to the hydroxyl O; the O−H and C_α−H distances are 1.16 and 1.57 Å, respectively. In the meantime, the hydroxyl oxygen and C_β atoms have approached each other with a O−C_β distance of 1.77 Å. The

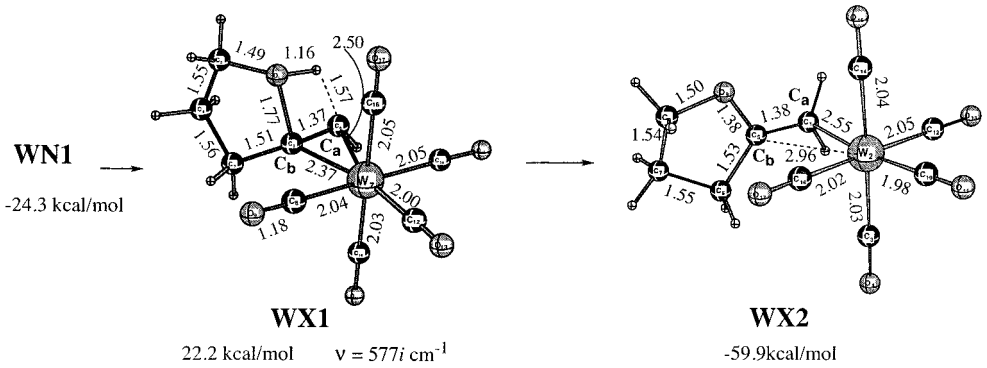

Figure 4. The optimized stationary point structures (in Å and deg) and relative energies (relative to $W(CO)_5$ + **1**) on the reaction pathway of *exo*-cycloisomerization of 4-pentyn-1-ol in the presence of the $W(CO)_5$ catalyst.

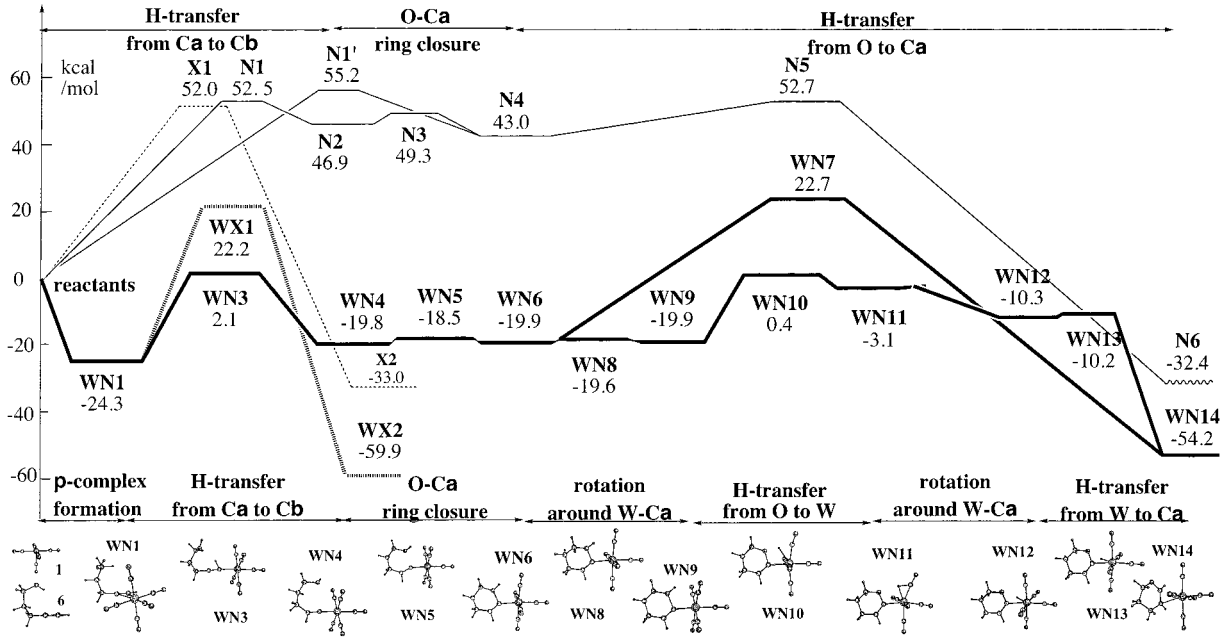

Figure 5. The overall energy potential profiles of cycloisomerization reactions of 4-pentyn-1-ol. (1) *endo*-Cycloisomerization with $W(CO)_5$: bold solid line with labels **WN1**−**WN13**. The natures of individual steps and the structures of intermediates and TSs are illustrated at the bottom of the figure. (2) *exo*-Cycloisomerization with $W(CO)_5$: bold broken line with labels **WX1**−**WX2**. (3) *endo*-Cycloisomerization without $W(CO)_5$: thin solid line with labels **N1**−**N6**. The natures of individual steps are illustrated at the top of the figure. (4) *exo*-Cycloisomerization without $W(CO)_5$: thin broken line with labels **X1**−**X2**.

$C_\alpha-C_\beta$ bond is elongated by 0.12 Å, from 1.25 Å in **WN1** to 1.37 Å in **WX1**. These geometrical parameters of TS **WX1** are very similar to those of its catalyst-free analogue **X1**, except for the $C_\alpha-C_\beta$ bond elongation that was only 0.09 Å in **X1**. A larger elongation of the $C_\alpha-C_\beta$ bond in **WN1** could be a result of its interaction with the W center. The normal coordinate analysis and pseudo-IRC calculation confirmed that this TS has one imaginary frequency of 577*i* cm^{-1}, which consists mainly of O → C_α hydride migration, O−C_β approach, and $C_\alpha-C_\beta$ stretch, and that it connects **WN1** with **WX2**. The activation barrier at **WX1** is calculated to be 46.5 kcal/mol, very much comparable to 52.0 kcal/mol for the catalyst-free process. In other words, the tungsten-catalyst has very little effect on the activation barrier of *exo*-cycloisomerization of 4-pentyn-1-ol. However, the tungsten-catalyst significantly increases the exothermicity of the *exo*-cycloisomerization process from 33.0 kcal/mol for catalyst-free to 59.9 kcal/mol for the catalyzed process. The increase of 25.5 kcal/mol is due to complexation of the *exo*-cycloisomerized product with $W(CO)_5$.

4. Conclusions

In the present paper, we have computationally studied and compared the reaction mechanisms of catalyst-free and tungsten-catalyzed *endo*- and *exo*-cycloisomerization of 4-pentyn-1-ol using B3LYP method with the basis sets of lanl2dz and SDD, for optimization geometries and energetics, respectively. The calculated potential energy profiles of all these processes are summarized in Figure 5. From these results and discussions we draw the following conclusions: (1) In the absence of the catalyst, both *endo*- and *exo*-cycloisomerizations of 4-pentyn-1-ol have very high activation barriers of 50−55 kcal/mol and are unlikely to be feasible. The catalyst-free *endo*-cycloisomerization process is a multistep reaction, the first step of which is hydride migration from the terminal carbon C_α to C_β to form a vinylidene intermediate, followed by ring-closure, and migration of hydride ligand from the hydroxyl ligand to C_α. The first step of the reaction is found to be rate-determining. Meanwhile, the catalyst-free *exo*-cycloisomerization is a single-step reaction and occurs via a concerted transition state.

(2) The pentacarbonyl tungsten catalyst does not significantly change either the mechanism or the energetics of *exo*-cycloisomerization reaction of 4-pentyn-1-ol. The reaction is a single-step reaction and proceeds via a large (47 kcal/mol) rate-determining barrier, which makes this process unfeasible.

(3) The presence of the tungsten catalyst makes the *endo*-cycloisomerization of 4-pentyn-1-ol much more complex but energetically much more accessible. The *endo*-cycloisomerization consists of many steps and proceeds with a rate-determining barrier of 26.4 kcal/mol, which is considerably lower than that for the catalyst-free process, and is feasible under mild experimental conditions. The first step of this reaction is coordination of substrate, 4-pentyn-1-ol, to the W center to form a π-complex **WN1**. The next step is the rate-determining step of the entire catalytic process, which involves migration of hydride from C_α to C_β via TS **WN3**, and produces the tungsten-vinylidene complex **WN4**. The most important role of the catalyst is to stabilize the intrinsically unstable vinylidene structure by forming a strong vinylidene−tungsten bond. The intermediate **WN4** rearranges to **WN6** with a six-membered ligand via a ring-closure TS **WN5** with a very small barrier. The resultant **WN6** goes through multiple W−C rotation and hydrogen migration steps and produces the final product complex **WN14**, with each of these steps occurring with low activation barriers. An interesting and more surprising feature of these multiple steps is that the carbonyl ligands and the transition metal participate in and mediate the overall hydride migration from the hydroxyl group to the C_α center; the hydride moves from the hydroxyl group initially to C(O), then to W, and finally to C_α. Obviously this mediation of hydride transfer is a second important role of the tungsten catalyst.

(4) The rate-determining barriers in the presence of the tungsten catalyst are 46.5 and 26.4 kcal/mol for the *exo*- and *endo*-cycloisomerization reactions, respectively, which clearly is the origin of the *endo*-regioselectivity of the cycloisomerization of the 4-pentyn-1-ol substrates reported experimentally. These calculated results support the experimentally proposed mechanism.[11]

(5) In the present study, we have not considered the effects of tertiary amine on the reaction mechanisms. Tertiary amines are always utilized in the experimental catalytic reaction. Considering the fact that the calculated rate-determining barrier for *endo*-cycloisomerization of 4-pentyn-1-ol in the presence of $W(CO)_5$ is still substantial (26.4 kcal/mol), one may suspect that amine is participating in the rate-determining step and further lowering the reaction barrier. We plan to study this problem soon.

Acknowledgment. The present research is in part supported by a grant (CHE96-27775) from the National Science Foundation (K.M.) and by a grant (CA-59703) from the National Cancer Institute (F.E.M.). Acknowledgment is made to the Cherry L. Emerson Center of Emory University for the use of its resources, which is in part supported by a National Science Foundation grant (CHE-0079627) and an IBM Shared University Research Award. Computer time allocated at the Center for Supercomputing Applications (NCSA) and Maui High Performance Computer Center (MHPCC) is also acknowledged.

Supporting Information Available: The optimized stationary point structures (in Å and deg) and relative energies (relative to $W(CO)_5$ + acetylene) for the adduct formation between acetylene and $W(CO)_5$, Cartesian coordinates for all stationary points, and total energies of all stationary points at each level of theory used in the paper (PDF). This material is available free of charge via the Internet at http://pubs.acs.org.

JA017668D